Effect of 9,9′-Bis(aryl)fluorene-modified Nanocellulose, Bamboo, and Bagasse Fibers on Mechanical Properties of Various Polymer Composites

Takumi Takeuchi,[a] Panuwat Luengrojanakul,[b] Hiroshi Ito,[c,d,*] Sarawut Rimdusit,[b] and Shinichi Shibata [a,*]

Impact-resistant automotive components were studied by evaluating the effects of single-screw and twin-screw extrusion on the mechanical properties of composites made from fluorene-modified nanocellulose (FCF) or bamboo fibers (30 wt%) combined with various polymers. Natural fiber composites were injection molded, and their mechanical properties were evaluated. Results showed that fluorene-modified nanocellulose exhibited improved dispersion when kneaded with polycarbonate and polyamide 6 using twin-screw extrusion, resulting in increases of over 5000 MPa in flexural modulus and over 40 MPa in maximum flexural stress compared to the base polymer. However, composites made with polyamide 66 and bamboo fibers required high injection molding temperatures exceeding 260 °C, which led to thermal degradation and reduced the fiber reinforcement effect on mechanical properties. The polypropylene showed weak interfacial compatibility with bamboo fibers, resulting in limited reinforcement effects in both single and twin-screw extrusion. The brittleness of the fibers did not significantly influence the elongation of the PP composite. Nonetheless, it exhibited less reduction in elongation compared to composites where bamboo or FCF was added to other polymers. Building on these results, flexural tests were conducted on composites combining high-impact polypropylene with natural fibers, demonstrating the potential for high-impact-resistant composite materials suitable for automotive applications.

DOI: 10.15376/biores.20.2.4136-4151

Keywords: Bamboo fiber; 9,9'-Bis(aryl)fluorene-modified nanocellulose; Green composite; Flexural properties; Plastic deformation

Contact information: a: Faculty of Engineering, Material Processing Laboratory, University of the Ryukyus, Nishihara 903-0213, Okinawa, Japan; b: Center of Excellence in Polymeric Materials for Medical Practice Devices, Department of Chemical Engineering, Chulalongkorn University, Bangkok, 10330, Thailand; c: Research Center for Green Materials and Advanced Processing, Yamagata University, 4-3-16 Jonan, Yonezawa, Yamagata 992-8510, Japan; d: Department of Organic Materials Science, Graduate School of Organic Materials Science, Yamagata University, 4-3-16 Jonan, Yonezawa, Yamagata 992-8510, Japan;

** Corresponding authors: ihiroshi@yz.yamagata-u.ac.jp; shibata@cs.u-ryukyu.ac.jp*

INTRODUCTION

Natural fiber composites are gaining attention as potential alternatives to petroleum-based materials, especially for automotive components (Naik *et al.* 2022). The advantages of natural fibers lie in their cost-effectiveness, lightweight nature, and high rigidity. Their specific gravity ranges from 1.2 to 1.5 g/cm³, and they exhibit tensile strengths and elastic moduli of up to 900 MPa and 80 GPa, respectively (Elfaleh *et al.* 2023). Through combining these lightweight, high-rigidity materials with resins and molding them, it is possible to contribute to the weight reduction of automotive components, potentially leading to improved fuel efficiency and reduced material costs

(Akampumuza *et al.* 2017; Suriani *et al.* 2021; Dua *et al.* 2023). However, there are significant drawbacks to natural fiber composites that cannot be overlooked. These include the reduced moldability of resins due to fiber incorporation and the occurrence of thermal degradation in resins, such as engineering plastics, when molded at high temperatures, which leads to a decrease in mechanical properties such as impact resistance, flexural strength and odor problems (Suriani *et al.* 2021). Improving the thermal properties of natural fiber composites is crucial when combined with thermoplastic polymers. Enhancing the thermal properties of natural fibers allows their use in composites with heat-resistant polymers such as PA6, enabling their application in engine compartments. The effects of various additives and fiber treatments on the thermal properties have been extensively studied by many researchers (Neto *et al.* 2021).

9,9'-Bis(aryl)fluorene, which has a bulky steric structure with cardo groups, shows high dispersibility and compatibility with resins. Fluorene-modified cellulose nanofibers have been developed, which possess fewer hydroxyl groups compared to conventional cellulose nanofibers or natural fibers, potentially offering higher heat resistance (Sugimoto *et al.* 2019; Sefat *et al.* 2021). The use of FCF and additives can expand the applications of natural fibers, but challenges such as cost and processability remain. Through combining these cellulose nanofibers with engineering polymers, the development of composite materials with exceptional mechanical properties is anticipated. However, considering the mechanical properties of natural fibers, which have low elongation, there is a possibility that the Charpy impact strength of natural fiber composites may decrease (Sobczak *et al.* 2012). Impact strength is a crucial property for automotive components, and stringent impact resistance standards are established for automotive resin parts, such as door trims to protect occupants in traffic accidents. Based on the authors' observations and experiences, an increase of Charpy impact strength of 5 kJ/m² for interior applications or 10 kJ/m² for exterior applications may be required for impact-resistant resin components, which is a challenging value even for neat polymers (Satoru *et al*. 2010). To the best of the authors' knowledge, no previous studies have investigated the application of fluorene-modified cellulose in automotive components, thus motivating this research. In this study, fiber-reinforced composites were developed by combining fluorene-modified nanocellulose, bamboo, and bagasse fibers with resins, aiming for their application in automotive components. Specifically, these fibers were incorporated into various resins commonly used in automotive parts, such as polypropylene (PP), bio-polycarbonate, Polyamide 6 (hereinafter referred to as PA 6), and polyamide 66 (PA 66). These materials are used for heat-resistant and interior automotive components, and they were selected to investigate their applicability in natural fiber composites. The composites were processed through injection molding, and their mechanical properties were evaluated. The target was set to achieve a flexural modulus of 5000 MPa and absorbed energy equivalent to an impact value exceeding 5 kJ/m².

EXPERIMENTAL

Materials and Methods

In this study, moso bamboo, naturally grown in the western part of Tokushima Prefecture, Japan, was used. The bamboo had a height of approximately 15 m, and the section of the bamboo culm ranging from 50 to 1000 mm from the ground was selected. To minimize errors in results due to the variability of natural fibers, only a single bamboo sample was used. The bamboo culm had a diameter of approximately 110 mm. The node portions were removed using a cutter, and the culm was cut into strips with a longitudinal

length of 70 mm and a circumferential length of 10 mm. Subsequently, the outer skin was peeled off with a cutter. These bamboo strips were placed in a flask and boiled in a 3% sodium hydroxide aqueous solution at 120 °C for 2 h in an oil bath. After this alkali treatment, the bamboo strips were washed with de-ionized water and dried in an electric oven at 60 °C for 24 h. The alkali-treated bamboo fiber strips were then finely ground using a grinder and sieved (ISO 3310-1 (2016), diameter 560 µm).

Bagasse fibers, the fibrous residue from sugarcane (hereafter referred to as "bagasse"), were supplied by a local sugar factory. These bagasse fibers were sieved to a size range of 5 to 20 mm to remove long fibers, pith, and particles. Except for being washed with hot water in the sugarcane mill, no chemical treatment was applied to these fibers. After being washed in hot water at 80 °C, the bagasse fibers were dried in an electric oven at 60 °C for 24 h, finely ground using a grinder, and sieved (ISO 3310-1 (2016), diameter 200 µm). Fluorene-modified cellulose nanofibers (FCF) were supplied by Osaka Gas Chemical Co., Ltd. (Osaka, Japan). The dried FCF was ground into a fine powder using an automatic stone mill. The polymers used in this study included polypropylene (PP(AZ864), Sumitomo Noblen, Japan, and PP(J762HP), Prime Polymer Co., Ltd., Japan), polyamide 6 (PA 6 A1030BRL, Unitika, Japan), polyamide 66 (PA66 Leona1300s, Asahi Kasei Corp., Japan), and isosorbide-based polycarbonate (Durabio D6350R, Mitsubishi Chemical, Japan).

Table 1. Composition and Processing Conditions of Polymer-Based Natural Fiber Composites

Material	Polymer (wt%)	Fiber	Fiber (wt%)	Extruder	Extruding temperature
PP(AZ864)(S)	100	-	0	Single	200
PP(AZ864)+FCF(S)	70	FCF	30	Single	200
PP(AZ864)+FCF(T)	70	FCF	30	Twin	200
PP(AZ864)+BF(S)	70	Bamboo	30	Single	200
PP(AZ864)+BF(T)	70	Bamboo	30	Twin	200
PP(J762HP)+BGF(T)	70	Bagasse	30	Twin	200
PC(S)	100	-		Single	230
PC+FCF(S)	70	FCF	30	Single	230
PC+FCF(T)	70	FCF	30	Twin	230
PC+BF(S)	70	Bamboo	30	Single	230
PC+BF(T)	70	Bamboo	30	Twin	230
PA6(S)	100	-		Single	240
PA6+FCF(S)	70	FCF	30	Single	240
PA6+FCF(T)	70	FCF	30	Twin	240
PA6+BF(S)	70	Bamboo	30	Single	240
PA6+BF(T)	70	Bamboo	30	Twin	240
PA66(S)	100	-		Single	280
PA66+FCF(S)	70	FCF	30	Single	280
PA66+FCF(T)	70	FCF	30	Twin	280
PA66+BF(S)	70	Bamboo	30	Single	280
PA66+BF(T)	70	Bamboo	30	Twin	280

In this study, the thermal stability and decomposition behavior of FCF were analyzed using a thermogravimetric analyzer (Mettler Toledo, TGA1, Switzerland). To simulate the thermal history during the pelletization and injection molding of FCF composites, isothermal conditions (210, 220, 230, 240, 250, 260, and 270 °C) were applied for 7 min, with measurements performed twice under nitrogen gas flow rate of 50 mL/min.

Mixtures of composite pellets (PP, PC, PA6, and PA66), along with FCF, bamboo fibers, and bagasse fibers, were compounded by melt blending using either a single-screw (L/D 30, 15 rpm for 2 minutes, S25, Orotrim Plastic Machinery Enterprise, China) or twin-screw (L/D 30, 200 rpm for 5 minutes, KZW15TW-30MG-NH, Technovel CO. Ltd., Japan) extruder, as shown in Table 1. The reason for comparing compounding methods for composites is that FCF consists of extremely fine fibers, which were expected to

exhibit differences depending on the blending method. The obtained strand compounds were cut into pellets with an average length of approximately 5 mm. These pellets were molded into test specimens using a 10-ton injection molding machine (type PS10E1ASE, Nissei Co. Ltd., Japan). Injection molding was performed at nozzle temperatures ranging from 170 to 270 °C, as shown in Table 2, with a holding pressure of 11 MPa, mold temperature of 60 °C, cooling time of 7 s, screw rotation speed of 50 rpm, and injection speed of 0.5 s/shot. The prepared composite specimens were cylindrical, with a diameter of 5.8 mm and a length of 60 mm.

The three-point flexural test was conducted in accordance with ISO 178 (2019), using at least five cylindrical specimens with a universal testing machine (EZ-SX, Shimadzu Co., Japan). The crosshead speed was set to 1 mm/min. The flexural modulus was determined from the first derivative of the load with respect to displacement in the load-displacement curve, with the differential range set at 0 to 15% of the maximum load. The flexural strength was calculated from the maximum load. Impact absorption energy is typically defined as the integral value of elastic and plastic deformation in impact testing; however, in this study, the amount of displacement and load in each flexural test was evaluated as the "absorbed energy." Although Charpy impact values and absorbed energy are not equivalent, they have a strong correlation, with the primary difference being the strain rate during testing (Cui *et al.* 2019; Ma *et al.* 2021).

The fracture surfaces of the flexural test specimens were observed using a scanning electron microscope (JEOL 6510A, Japan). Before observation, the specimens were coated with gold (JFC-1100; JEOL, Tokyo, Japan). The accelerating voltage was set at 5 kV.

RESULTS AND DISCUSSION

Figure 1 shows the relationship between the weight loss percentage and the heating temperature for FCF and bamboo in thermogravimetric analysis (TGA). Overall, as the heating temperature increased, the weight loss tended to rise. The weight loss increased with increasing temperature, with significant weight loss observed at holding temperature above 250 °C. The high temperature processing resulted in the thermal degradation of fiber structure, loosening of the cell wall, and generation of pores (Cui *et al.* 2023). The weight loss in the second stage was lower than in the first stage. It was found that at heating temperatures above 240 °C, the weight loss of FCF was significantly lower than that of bamboo. This is likely due to the substitution of hydroxyl groups in the fibers with fluorine (Sugimoto *et al.* 2019). In the authors' previous paper (Takeuchi *et al.* 2023), it was reported that bamboo heated at temperatures above 250 °C exhibited a reduction in strength of more than 50% compared to heating at 210 °C. Therefore, it is expected that the strength of the composite material will significantly decrease when the molding temperature exceeds 250 °C. This degradation phenomenon corresponds to the relationship between the weight loss rate and temperature shown in Fig. 2, indicating that once thermal decomposition progresses beyond a weight loss of 6%, the structural components of natural fibers, such as lignin and hemicellulose, start to degrade (Thomason and Rudeiros-Fernández 2021). In this way, when natural fibers are heated at high temperatures, they decompose into substances such as carbon monoxide, methane, hydrogen, carbon dioxide, formaldehyde, water, methanol, ketene, and acetic acid (Thomason and Rudeiros-Fernández 2021). Consequently, heating above 250 °C gradually damages the fiber skeleton, leading to a significant decrease in mechanical properties.

Figures 2 (a through h) show the load-displacement curves for various composite materials and polymers. In these figures, the symbols "S" and "T" represent pellets produced using single-screw and twin-screw extrusion, respectively.

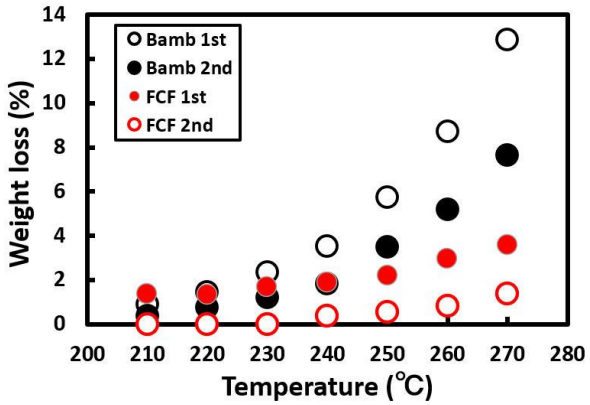

Fig. 1. Relationship between temperature on isothermal thermogravimetric analysis and mass loss percentage in FCF and bamboo fiber

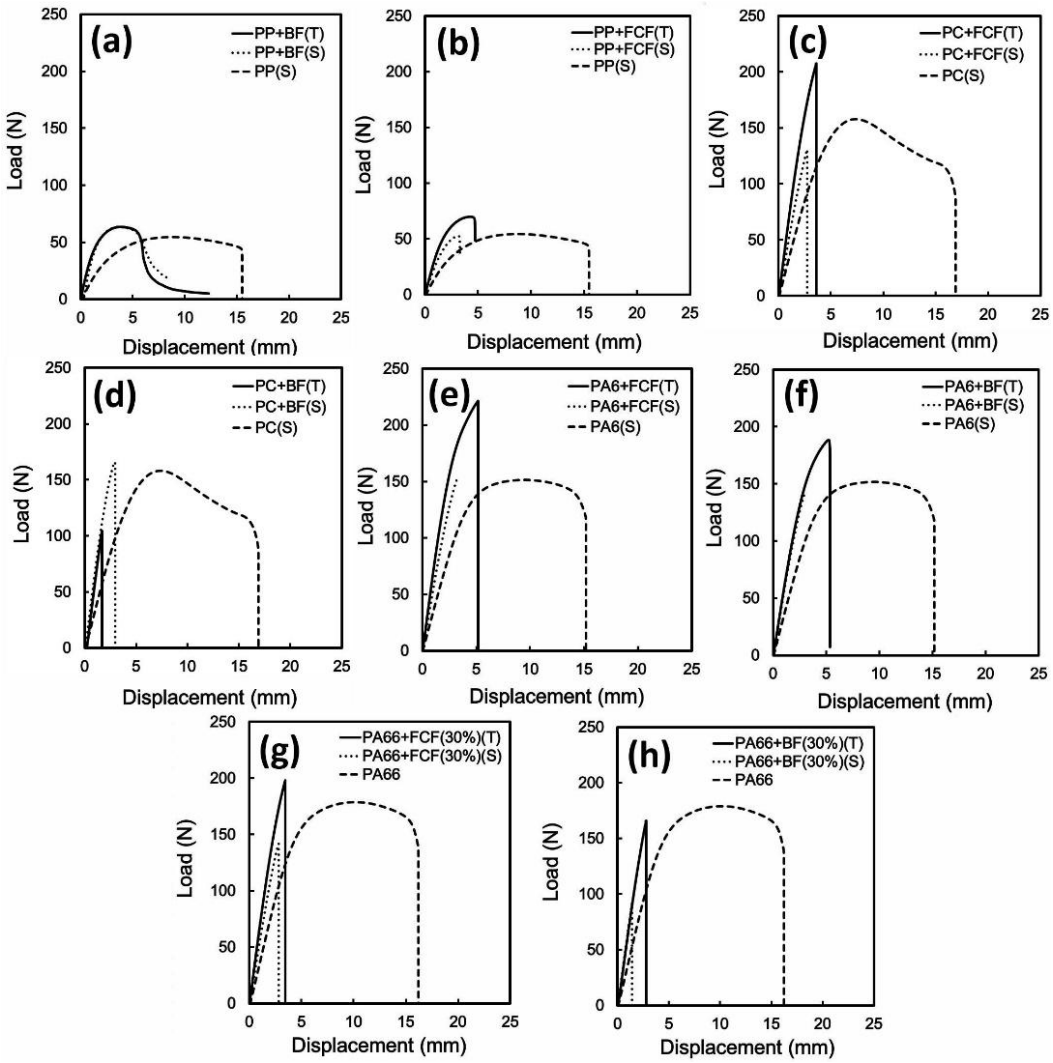

Fig. 2. Flexural load-displacement curves of fiber-reinforced composites at 30 wt% bamboo and FCF fibers: (a) PP+bamboo, (b) PP+FCF, (c) PC+bamboo, (d) PC+FCF, (e) PA6+bamboo, (f) PA6+FCF, (g) PA66+bamboo, and (h) PA66+FCF

Table 2 summarizes the experimental results. First, the effects of single-screw and twin-screw extrusion methods on flexural modulus and stress are considered. Specimens blended using a twin-screw extruder (especially PC, PA6, and PA66) exhibited significantly higher flexural modulus and flexural strength compared to those mixed with a single-screw extruder.

The FCF composites showed notable improvements in mechanical properties when compounded with a twin-screw extruder. Because FCF is composed of nanocellulose, the twin-screw mixing process may have improved the dispersion of fibers within the matrix resins. In twin-screw compounding, the screw rotation speed was 200 rpm for 5 min, whereas in single-screw compounding, it was 30 rpm for 2 min. The degree of mixing differed significantly between the two methods, which is considered to have influenced the experimental results. Therefore, fracture surface observations were conducted using a scanning electron microscope. Figures 3(a through d) show the fracture surfaces after flexural testing for composites containing bamboo or FCF mixed with polypropylene. Figures 3(a) and (c) show polypropylene composites mixed with bamboo and FCF using a single-screw extruder, while Fig. 3(b) and (d) show polypropylene composites mixed with a twin-screw extruder. In Fig. 3(a) and (c), relatively large clumps of bamboo fibers and FCF are observed. In contrast, Fig. 3(b) shows crushed bamboo fibers with relatively small diameters, and Fig. 3(d) shows that although some small clumps of FCF remain, overall, the FCF is well-dispersed. Despite the improved dispersion of FCF in polypropylene, the increase in mechanical properties of the composite was smaller compared to other polymers, which may be attributed to poor compatibility between FCF and polypropylene (PP).

Table 2. Mechanical Properties of Bamboo and FCF Polymer Composites under Various Processing Conditions

Material	Injection molding temperature (°C)	Load N Mean (SD)	Flexural modulus (MPa) Mean (SD)	Increment in flexural modulus (MPa)	Max. flexural stress (MPa) Mean (SD)
PP(AZ864)(S)	170	56 (1.13)	1307 (71.1)	—	40 (1.31)
PP(AZ864)+FCF(S)	170	53 (3.37)	1923 (98.3)	616	36 (2.04)
PP(AZ864)+FCF(T)	170	66 (3.70)	2417 (43.4)	1110	46 (1.51)
PP(AZ864)+BF(S)	170	67 (4.34)	3695 (212)	2388	46 (1.88)
PP(AZ864)+BF(T)	170	62 (1.77)	2991 (73.7)	1684	43 (0.91)
PC(S)	230	168 (2.00)	3057 (41.1)	—	105 (1.13)
PC+FCF(S)	230	124 (6.46)	4148 (98.5)	1091	82 (4.44)
PC+FCF(T)	230	200 (7.99)	7482 (229)	4425	135 (5.82)
PC+BF(S)	230	161 (3.37)	5808 (367)	1660	106 (2.19)
PC+BF(T)	230	132 (23.5)	5484 (505)	1336	87 (15.5)
PA6(S)	240	156 (2.25)	3152 (40.6)	—	106 (1.07)
PA6+FCF(S)	250	148 (3.78)	4766 (73.1)	1614	101 (2.82)
PA6+FCF(T)	250	216 (4.25)	8178 (222)	5026	152 (2.87)
PA6 + BF(S)	250	135 (16.5)	4686 (31.3)	1534	91 (11.1)
PA6+BF(T)	250	164 (14.3)	4868 (542)	1716	112 (8.91)
PA66(S)	260	178 (4.15)	4015 (118)	—	126 (5.13)
PA66+FCF(S)	260	136 (7.61)	4451 (157)	436	94 (5.54)
PA66+FCF(T)	260	185 (10.5)	6858 (499)	2843	128 (7.83)
PA66+BF(S)	270	86 (6.86)	4716 (148)	701	59 (4.54)
PA66+BF(T)	270	164 (3.78)	5926 (247)	1911	113 (2.81)

The absorbed energy of the bamboo-PP (AZ864) composite material decreased significantly compared to the base PP (AZ864). The percentage values in the far-right column of Table 3 represent the relative absorbed energy of the composites, assuming the base material's absorbed energy is 100%. Generally, fibers have extremely low elongation, and when bamboo fibers are mixed with polymers, the brittleness of the fibers significantly impacts the absorbed energy of the composite, causing a substantial

decrease. If the interface between the fibers and the resin is not well bonded, the fibers may act as defects. However, absorbed energy can be a critical property for automotive components, especially for parts that may be subjected to collisions or impacts, where strict impact strength standards are established. Based on the authors' knowledge, the impact resistance requirement for automotive components typically specifies Charpy impact values of 5 kJ/m² or more, or 10 kJ/m² or more. Although these are stringent standards, the absorbed energy of the bamboo-PP (AZ864) composite material kneaded with a twin-screw extruder reached 54% of the base material. This value was the highest in Table 3. As shown in Fig. 2(a), the weak interfacial adhesion between the natural fibers and PP (AZ864) may have contributed to its ductility. From this perspective, using a PP base material with excellent impact properties suggests the possibility of exceeding these stringent standards with bagasse-PP composites. Therefore, as described later, a PP with significantly higher impact strength was selected to fabricate bamboo-PP composites. Additional experiments were conducted, and the results were verified.

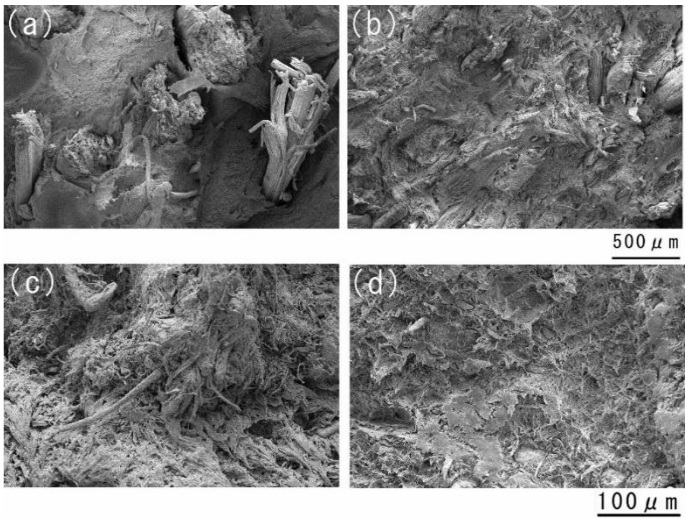

Fig. 3. SEM micrographs of fractured composite surfaces: (a) PP+bamboo (S), (b) PP+bamboo (T), (c) PP+FCF (S), and (d) PP+FCF (T); (S) single extruder and (T) twin extruder SEM micrographs of (a) (b)

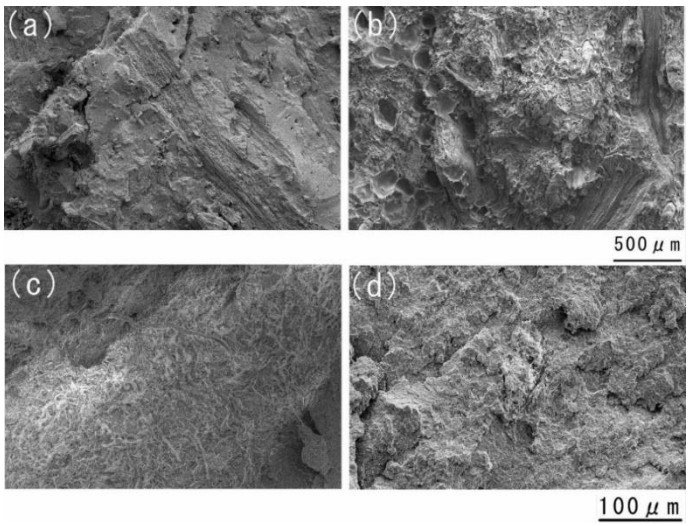

Fig. 4. SEM micrographs of fractured composite surfaces: (a) PA6+bamboo (S), (b) PA6+bamboo (T), (c) PA6+FCF (S), and (d) PA6+FCF (T); (S) single extruder and (T) twin extruder SEM micrographs of (a) (b)

Next, the mechanical properties of composite materials mixed with FCF or bamboo into PC and PA6 are discussed. The measurement results of these composites were very similar to each other. Significant differences were observed in the results of materials mixed using single-screw and twin-screw extruders, particularly regarding FCF. The composite materials based on PC and PA6 mixed with a single-screw extruder showed increases in flexural modulus of 1091 and 1614 MPa, respectively, whereas those mixed with a twin-screw extruder demonstrated substantial increases to 4425 and 5026 MPa, respectively. These results suggest that mixing with a twin-screw extruder greatly improved the dispersion state of FCF within the base resin. In contrast, when bamboo was mixed with PA6 using both single-screw and twin-screw extruders, the increase rates of flexural modulus and flexural strength were found to be lower compared to PP (AZ864) in either case.

PC and PA6 were molded at injection temperatures of 230 and 250 °C, respectively. At these temperatures, as shown in Fig. 1, thermal decomposition of the bamboo fibers likely progressed during the material mixing and injection molding processes, leading to partial decomposition of the bamboo fiber structure. Figures 4(a) to (d) show SEM images of the fracture surfaces of composite specimens containing bamboo fibers or FCF mixed with PA6 after flexural testing. For bamboo fibers, it was observed that composites mixed with a twin-screw extruder exhibited more finely crushed bamboo fibers compared to those mixed with a single-screw extruder.

However, as indicated in Table 2, there was almost no significant difference in flexural strength or flexural modulus between the composites mixed with a single-screw extruder and those mixed with a twin-screw extruder. This is thought to be due to the simultaneous occurrence of positive factors, such as improved dispersion of the bamboo fibers, and negative factors, such as shortening of the fiber length due to fragmentation. Regarding FCF, as seen in Figs. 4(c) and (d), there was a marked difference in the dispersion of FCF between the composites mixed with a single-screw extruder and those mixed with a twin-screw extruder. In the former, clumps of FCF were observed in many areas, while in the latter, FCF was uniformly dispersed within the matrix polymer (PA6) to the point where the boundary between the FCF and the base polymer was no longer discernible. This fine and homogeneous dispersion of FCF is believed to have significantly improved the flexural strength and flexural modulus, as shown in Table 2.

Finally, let us consider PA66. The composite materials of PA66 with bamboo fibers and FCF exhibited relatively modest increases in flexural strength and flexural modulus compared to the base resin. For FCF, the increase in flexural modulus relative to the base material was 436 MPa for the single-screw extruder composite and 2834 MPa for the twin-screw extruder composite. Similarly, for bamboo fibers, these values were 701 MPa and 1911 MPa, respectively. Because PA66 was injection molded at a high temperature of 270 °C, which promotes thermal decomposition of bamboo fibers, it is presumed that the structures of both the bamboo fibers and the FCF were significantly degraded by thermal decomposition, as indicated in Table 2.

In the previous section, it was reported that the absorbed energy of polymer composites mixed with FCF or bamboo fibers significantly decreased. The PP (AZ864, Charpy impact strength 9 kJ/m²) used in the previous experiments is a material designed for impact resistance; however, when mixed with plant fibers, it may fail to meet the automotive impact component standards of 5 kJ/m² or 10 kJ/m². Therefore, experiments were conducted to improve the absorbed energy of plant fiber composites, with the goal of developing impact-resistant automotive components.

In this section, bagasse, a byproduct of sugarcane, was used instead of bamboo or FCF. This decision was because the production cost of FCF is currently 50 to 100 times higher than that of bagasse, and bamboo is difficult to procure in stable and large

quantities. In contrast, bagasse is available in large quantities throughout the year from sugar mills and is easy to obtain. Furthermore, life cycle assessments have validated bagasse as a viable alternative to talc. Considering these factors, bagasse was selected as the reinforcing fiber material (Luz *et al.* 2010).

Figure 5 (a through f) shows the load-displacement curves of bagasse-PP (AZ864) composites kneaded and injection-molded with varying bagasse fiber contents. Table 3 summarizes the numerical results from Fig. 6. As the bagasse weight ratio increases, it becomes more difficult to mix with the resin, making it necessary to increase the compounding temperature. As evident from Fig. 5, increasing the weight ratio of bagasse fibers significantly reduced the elongation of the composites. Variations in elongation were observed among specimens tested with bagasse fiber composites. When the bagasse content increased to 10%, 20%, and 30%, the absorbed energy decreased to 92%, 48%, and 43%, respectively, compared to the base AZ864. The significant variation in elongation at 10% bagasse content may be attributed to non-uniform fiber distribution within the specimen.

In this study, the Charpy impact strength target for composite materials used in automotive impact-resistant parts was set at 5 kJ/m² or 10 kJ/m². To achieve this, an additional experiment was conducted to investigate whether using PP (J762HP, Charpy impact strength of 14 kJ/m²), which has higher impact strength, could improve the impact resistance. Figures 6(a) and (b) show the load-displacement curves of flexural tests for injection-molded specimens with 30 wt% bagasse fibers added to AZ864 and J762HP, respectively. Table 4 summarizes the numerical results. As shown in Fig. 7 and Table 4, the bagasse-PP (J762HP) composites exhibited similar flexural stress and flexural modulus compared to the bagasse-AZ864 composites, but the elongation increased significantly. Assuming equivalence between absorbed energy and impact strength, the Charpy impact value for PP (J762HP) was estimated to range from 4.2 kJ/m² to 11.4 kJ/m².

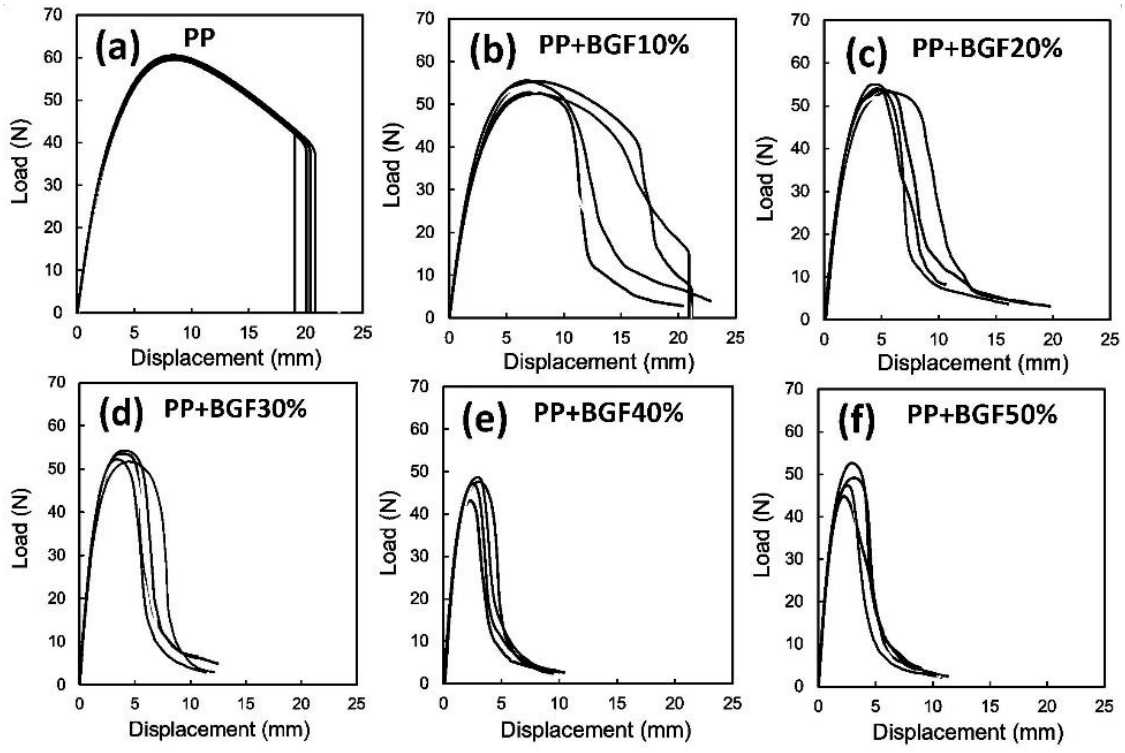

Fig. 5. Flexural load-displacement curves of bagasse fiber-reinforced composites: (a) 0 wt%, (b) 10 wt%, (c) 20 wt%, (d) 30 wt%, (e) 40 wt% and (f) 50 wt%

Table 3. Flexural Properties and Energy Absorption of Bagasse-PP Composites with Varying Fiber Content

Material	Injection molding temperature (°C)	Load N Mean (SD)	Flexural modulus (MPa) Mean (SD)	Increment in flexural modulus (MPa)	Max. flexural stress (MPa) Mean (SD)	Absorbed energy (%)
PP(AZ864)	170	56 (1.13)	1307 (71.1)	—	40 (1.31)	100%
PP(AZ864)+BGF10%	170	55 (0.75)	1406 (52.4)	99	37 (0.75)	92%
PP(AZ864)+BGF20%	170	54 (0.97)	1822 (58.5)	515	37 (0.60)	48%
PP(AZ864)+BGF30%	260	53(0.89)	2119 (72.1)	812	36 (0.89)	43%
PP(AZ864)+BGF40%	270	47 (2.32)	2419 (103.7)	1112	32 (1.81)	24%
PP(AZ864)+BGF50%	270	49 (2.63)	2425 (46.4)	1118	33 (1.89)	31%

To further analyze this behavior, flexural tests were temporarily paused near the maximum load, and the central tensile portion of the bagasse-PP (J762HP) composite specimens was observed using an optical microscope. After fracture, the same region was re-examined and compared. The observations are shown in Figs. 8(a-d). The center of all images corresponds to the central tensile side of the specimen. Figures 8(a) and (c) are microscopic images of cases with very low elongation (fracture at 13 mm), while Figs. 8(b) and (d) represent cases with high elongation (fracture at 19 mm). As seen in the images, specimens with low elongation (a) exhibited concentrated plastic strain (white vertical lines) at the center near the maximum load. The fewer the white lines, the more localized the plastic strain. In contrast, specimens with high elongation during the flexural test displayed more white vertical lines, indicating that the plastic strain was distributed around the maximum load point. These observations suggest that variations in fiber distribution within the injection-molded specimens caused the differences in elongation.

In the previous section, it was reported that the absorbed energy of polymer composites mixed with FCF or bamboo fibers significantly decreased. The PP (AZ864, Charpy impact strength 9 kJ/m²) used in the previous experiments is a material designed for impact resistance; however, when mixed with natural fibers, it may fail to meet the automotive impact part standards of 5 kJ/m² or 10 kJ/m². Therefore, additional experiments were conducted to improve the absorbed energy of natural fiber composites. In this section, bagasse, a byproduct of sugarcane, was used instead of bamboo. Bagasse was selected as a reinforcing material because it is abundantly available, easy to procure, suitable for automotive applications, and a viable alternative to talc from a life cycle assessment perspective.

Figure 5 (a through f) shows the load-displacement curves of bagasse-PP (AZ864) composites kneaded and injection-molded with varying bagasse fiber content. Table 3 summarizes the numerical results from Fig. 6. As evident from Fig. 5, increasing the weight ratio of bagasse fibers significantly reduced the elongation of the composites. Moreover, noticeable variations in elongation were observed in the bagasse fiber composites across tests. When the bagasse content was increased to 10%, 20%, and 30%, the absorbed energy decreased to 92%, 48%, and 43%, respectively, compared to the base AZ864. The large variation in elongation at 10% bagasse content may be due to non-uniform fiber distribution within the specimens. In this study, the Charpy impact strength target for composites used in automotive impact-resistant parts was set at 5 or 10 kJ/m². To achieve this, an experiment was conducted using PP (J762HP, Charpy impact strength 14 kJ/m²), which has higher impact strength, to investigate whether the impact resistance could be improved. Figures 7(a) and (b) show the load-displacement curves for flexural tests of injection-molded specimens containing 30wt% bagasse fibers in AZ864 and J762HP, respectively. Table 3 summarizes the numerical results of these experiments. As shown in Fig. 7 and Table 3, the bagasse-PP (J762HP) composite exhibited similar

flexural stress and flexural modulus to the bagasse-AZ864 composite but demonstrated a significant increase in elongation. Assuming equivalence between absorbed energy and impact strength, the Charpy impact strength of PP (J762HP) is estimated to range from 4.2 kJ/m² to 11.4 kJ/m².

In the previous section, it was mentioned that the impact strength of polymer composites significantly decreases when compounded with FCF or bamboo. The PP (AZ864) used in the previous section is designed for impact resistance; however, when mixed with natural fibers, it may not meet the automotive impact-resistant component standards of 5 kJ/m² or more, or even 10 kJ/m². Therefore, additional experiments were conducted to improve the impact values of natural fiber composite materials. In this section, bagasse, a byproduct of sugarcane, was used instead of bamboo. Bagasse is abundant and easily available, making it suitable for automotive parts applications. From a life cycle assessment perspective, it is considered a material that can replace talc. Taking these factors into account, bagasse was selected as the reinforcing fiber (Luz *et al.* 2010).

Figures 6 (a through f) show the load-displacement curves of bagasse-PP (AZ864) composites with different bagasse fiber contents, compounded and injection-molded. Table 2 summarizes the numerical test results presented in Fig. 6. As shown in Fig. 5, increasing the bagasse fiber content significantly reduced the elongation of the composite materials. Additionally, the bagasse fiber composites exhibited relatively large variations in elongation during each test. When the bagasse content was increased to 10%, 20%, and 30%, the impact strength decreased to 8.3 kJ/m² (92%), 4.3 kJ/m² (48%), and 3.9 kJ/m² (43%) of the base PP (AZ864) resin's impact strength, respectively. In this study, the target Charpy impact strength for composite materials used in automotive impact-resistant parts was set at 5 kJ/m² or more, with a goal of achieving 10 kJ/m². Therefore, experiments were conducted to investigate whether the impact strength could be improved using PP (J762HP, Charpy impact strength of 14 kJ/m²), which has a higher impact strength than PP (AZ864).

Figures 6(a) and (b) show the load-displacement curves of injection-molded test specimens with 30 wt% bagasse fibers added to AZ864 and J762HP, respectively, during flexural tests. Table 3 summarizes the numerical results of these experiments. As shown in Fig. 7 and Table 3, compared to the bagasse-PP (AZ864) composites, the bagasse-PP (J762HP) composites exhibited similar flexural stress and flexural modulus but significantly increased elongation. However, there was considerable variation in elongation. The impact strength ranged between 4.2 kJ/m² and 11.4 kJ/m².

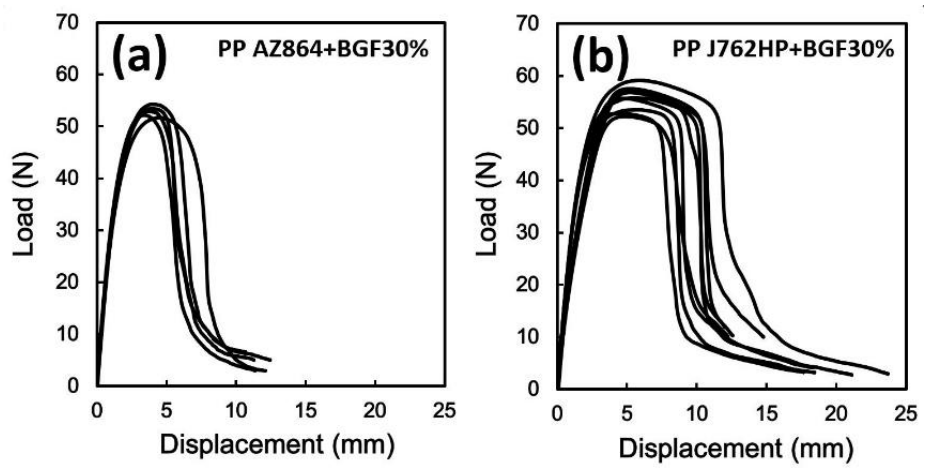

Fig. 6. Flexural load-displacement curves of fiber-reinforced composites at 30 wt% bagasse fibers: (a) PP (AZ864) + bagasse and (b) PP (J762HP) + bagasse

Table 4. Flexural Properties and Energy Absorption of Bagasse-PP Composites with 30% Fiber Content: Comparison Between PP(AZ864) and PP(J762HP)

Material	Injection molding temperature (°C)	Load N Mean (SD)	Flexural modulus (MPa) Mean (SD)	Max. flexural stress (MPa) Mean (SD)	Absorbed energy (%)
AZ864	170	56 (1.13)	1307 (71.1)	40 (1.31)	100%
AZ864+BGF30%-1	170	53	2068	36	43%
AZ864+BGF30%-2	170	54	2081	36	45%
AZ864+BGF30%-3	170	53	2073	35	41%
AZ864+BGF30%-4	170	52	2117	35	50%
AZ864+BGF30%-5	170	52	2260	35	38%
Ave. (SD)	170	53(0.89)	2120(72.1)	36(0.44)	43%
J762HP	170	55.2(0.51)	1159(40)	38.5(0.83)	100%
J762HP+BGF30%-1	170	53	2067	36	51%
J762HP+BGF30%-2	170	53	2260	37	48%
J762HP+BGF30%-3	170	59	2113	40	81%
J762HP+BGF30%-4	170	61	2193	39	64%
J762HP+BGF30%-5	170	51	2123	35	30%
Ave. (SD)	170	55.3(2.73)	2158(67.6)	38.2(1.74)	61%

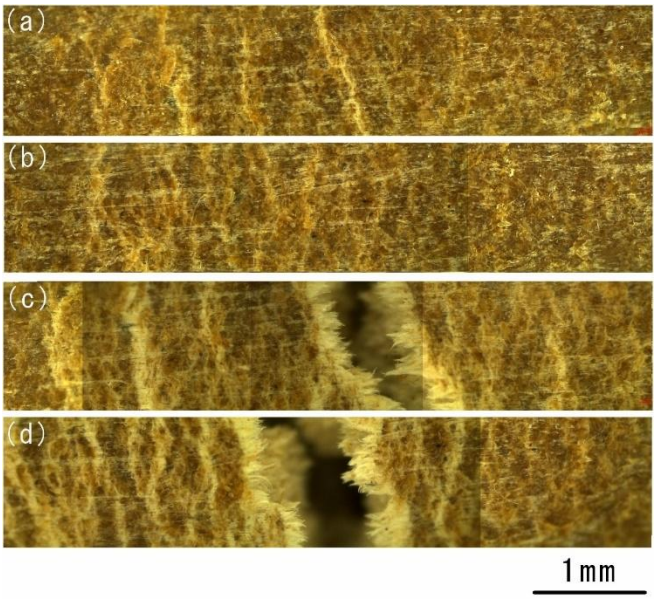

Fig. 7. Optical micrographs of composite surfaces on the tensile side: (a, b) during flexural testing and (c, d) after, with low (a, c) and high (b, d) elongation

For further analysis, during the flexural test, the test was temporarily interrupted near the maximum load, and the central tensile part of the bagasse-PP (J762HP) composite specimens were observed under an optical microscope. After fracture, the same region was photographed and compared. The results of these observations are shown in Fig. 7 (a through d). The center of all images corresponds to the central tensile region of the specimen. Figures 7(a) and (c) show microscopic images of cases with very low elongation (fractured at 13 mm), while Fig. 7(b) and (d) show cases with high elongation (fractured at 19 mm). As shown in the images, specimens with low elongation (a) exhibited concentrated plastic strain (white vertical lines) near the center at the maximum load. Fewer white lines meant the plastic strain was more localized. In contrast, specimens that exhibited higher elongation during the flexural test displayed a greater

number of white vertical lines, indicating that the plastic strain was more distributed near the maximum load point. These results suggest that variations in fiber distribution within the injection-molded specimens caused the observed differences in elongation.

To investigate the variability of bagasse fibers within pellets, 20 pellets were randomly selected and hot-pressed at 200 °C to produce films with a thickness of 0.2 mm. Figure 8 shows an image of the produced films. The white particles visible in the photo represent bagasse fibers. After hot pressing, the resin spread thinly and circularly, but the bagasse fibers did not disperse uniformly, showing uneven distribution. Approximately 10 films were prepared, all yielding similar results. These experimental results suggest that fluctuations in bagasse fiber concentration may also occur during the flow of bagasse-polymer mixtures in injection molding. In the flexural test, the elongation behavior of bagasse-PP composites varied significantly between specimens, with notable differences observed in each case. At present, it is unclear whether this uneven dispersion of bagasse is due to inhomogeneity within the pellets or uneven dispersion during flow in the mold. Additionally, the uneven distribution of bagasse might have occurred during mixing in the screw of the injection molding machine.

To investigate the variation of bagasse fibers within pellets, 20 pellets were randomly selected and hot-pressed at 200 °C to produce films with a thickness of 0.2 mm. Figure 8 shows an image of the films. The white particles visible in the photo are bagasse fibers. After hot pressing, the resin spread thinly and circularly, but the bagasse fibers did not spread uniformly, showing uneven dispersion. It is anticipated that the concentration of bagasse fibers may fluctuate during injection molding, influenced by the flow of the bagasse-polymer mixture. In the flexural test, the elongation behavior of the bagasse-PP composite material varied significantly. At present, it is unclear whether this uneven distribution of bagasse is due to the inhomogeneity of the bagasse within the pellets or whether it occurs due to the flow in the mold.

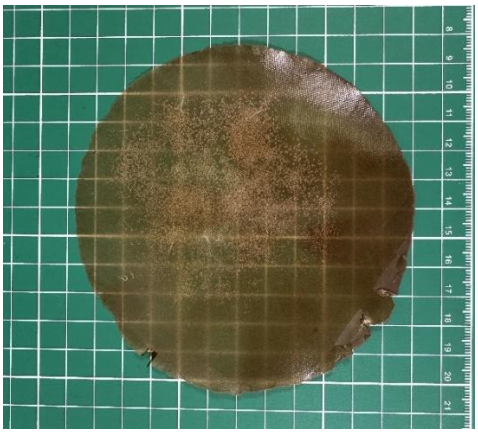

Fig. 8. The film structure after hot pressing of the pellets

Several studies have been conducted on fiber segregation and orientation within molds during injection molding. It has been reported that skin and core layers may form within the mold, and that fiber anisotropy and density can vary greatly depending on the location within the mold. Factors such as fiber length, injection speed, molding conditions, and rheology, have also been reported to influence fiber distribution within injection-molded parts (Nyström 2007; Papathanasiou *et al.* 2022).

Going forward, detailed investigations into the flow behavior of natural fibers within molds will be necessary to achieve homogeneous natural fiber composite injection-molded products. Such in-depth studies are considered essential for expanding the application of natural fiber materials in automotive impact-resistant components.

CONCLUSIONS

1. Thermogravimetric analysis (TGA) of bamboo and fluorine modified nanocellulose (FCF) revealed that FCF exhibited significantly higher heat resistance compared to bamboo. This result is attributed to the substitution of hydroxyl groups on the surface of nanocellulose with fluorene, which suppressed thermal degradation reactions at the same temperature.
2. The FCF showed a greater reinforcing effect when kneaded with a twin-screw extruder compared to a single-screw extruder. This effect was particularly pronounced in PC and PA6, where the flexural modulus exceeded 7000 MPa and the flexural strength surpassed 130 MPa. However, the addition of FCF or bamboo significantly reduced elongation, and the absorbed energy fell to below 40% of the base material, making them unsuitable for impact-resistant automotive components.
3. To meet the Charpy impact strength requirement for automotive impact-resistant components of 5 kJ/m² or 10 kJ/m² or more, a mixture of impact-resistant PP J762HP and 30% bagasse powder was injection-molded. Some specimens showed results that may exceed the standard. However, there was considerable variation in elongation among the specimens. Specimens exhibiting high absorbed energy showed uniform elongation at the center of the tensile side, while those with low absorbed energy exhibited localized plastic strain.

Therefore, further detailed investigations into the dispersion state of natural fibers within pellets or the flow of natural fibers within the mold are likely to lead to the development of more uniform natural fiber composite materials. Achieving this could allow the production of natural fiber composite materials suitable for automotive impact-resistant components.

ACKNOWLEDGEMENTS

The authors would like to thank Prof. Sanong Ekgasit at the Department of Chemistry, Faculty of Science, Chulalongkorn University for SEM experiments. S.R. and P.L. would like to acknowledge the financial supports from National Research Council of Thailand (NRCT) and Chulalongkorn University (N42A660910) and from Thailand Science Research and Innovation Fund Chulalongkorn University (BCG_FF_68_206_2100_030).

REFERENCES CITED

Akampumuza, O., Wambua, P. M., Ahmed, A., Li, W., and Qin, X. H. (2017). "Review of the applications of biocomposites in the automotive industry," *Polymer Composites* 38(11), 2553-2569. DOI: 10.1002/pc.23847

Cui, J., Fu, D., Mi, L., Li, L., Liu, Y., Wang, C., He, C., Zhang, H., Chen, Y., and Wang, Q. (2023). "Effects of thermal treatment on the mechanical properties of bamboo fiber bundles," *Materials* 16(3), article 1239. DOI: 10.3390/ma16031239

Cui, J., Wang, S., Wang, S., Li, G., Wang, P., and Liang, C. (2019). "The effects of strain rates on mechanical properties thermoplastic composites," *Polymers* 11(12), article 2019.

Dua, S., Khatri, H., Naveen, J., Jawaid, M., Jayakrishna, K., Norrrahim, M. N. F., and Rashedi, A. (2023). "Potential of natural fiber based polymeric composites for

cleaner automotive component production – A comprehensive review," *Journal of Materials Research and Technology* 25, 1086-1104. DOI: 10.1016/j.jmrt.2023.06.019

Elfaleh, I., Abbassi, F., Habibi, M., Ahmad, F., Guedri, M., Nasri, M., and Garnier, C. (2023). "A comprehensive review of natural fibers and their composites: An eco-friendly alternative to conventional materials," *Results in Engineering* 19, article ID 101271. DOI: 10.1016/j.rineng.2023.101271

ISO 3310-1 (2016). "Specifies the technical requirement and corresponding test methods for test sieves of metal wire cloth," International Organization for Standardization, Geneva, Switzerland.

ISO 178 (2019). "Plastics – Determination of flexural properties," International Organization for Standardization, Geneva, Switzerland.

Luz, S. M., Caldeira-Pires, A., and Ferrão, P. M. C. (2010). "Environmental benefits of substituting talc by sugarcane bagasse fibers as reinforcement in polypropylene composites: Ecodesign and LCA as strategy for automotive components," *Resources, Conservation and Recycling* 54(12), 1135-1144. DOI: 10.1016/j.resconrec.2010.03.009

Ma, L., Liu, F., Liu, D., and Liu, Y. (2021). "Review of strain rate effects of fiber-reinforced polymer composites," *Polymers* 13(17), article 2839. DOI: 10.3390/polym13172839

Naik, V., Kumar, M., and Kaup, V. (2022). "A review on natural fiber composite materials in automotive applications," *Engineered Science* 18, 1-10. DOI: 10.30919/es8d589

Neto, J. S. S., de Queiroz, H. F. M., Aguiar, R. A. A., and Banea, M. D. (2021). "A review on the thermal characterisation of natural and hybrid fiber composites," *Polymers* 13(24), article 4425. DOI: 10.3390/polym13244425

Nyström, B. (2007). "Natural fiber composites: Optimization of microstructure and processing parameters," *Department of Applied Physics and Mechanical Engineering* 15(4), 281-285.

Papathanasiou, T. D., Kuehnert, I., and Polychronopoulos, N. D. (2022). "Flow-induced alignment in injection molding of fiber-reinforced polymer composites," in: *Flow-Induced Alignment in Composite Materials*, Woodhead Publishing, Sawston, UK, pp. 123-185. DOI: 10.1016/B978-0-12-818574-2.00001-4

Satoru, M., Tsuyoshi, W., and Susumu, K. (2010). *Polypropylene Compounds for Automotive Applications*, Sumitomo Kagaku R&D report, Tokyo, Japan (English Edition.

Sefat, K. M., Kurose, T., Yamada, M., Ito, H., and Shibata, S. (2021). "Fabrication of 9,9′-Bis(aryl)fluorene-modified nanocellulose bamboo fiber composite," *BioResources* 16(2), 3907-3915. DOI: 10.15376/biores.16.2.3907-3915

Sobczak, L., Lang, R. W., and Haider, A. (2012). "Polypropylene composites with natural fibers and wood - General mechanical property profiles," *Composites Science and Technology* 72(5), 550-557. DOI: 10.1016/j.compscitech.2011.12.013

Sugimoto, M., Yamada, M., Sato, H., and Tokumitsu, K. (2019). "Reinforcement of polyamide 6/66 with a 9,9′-bis(aryl)fluorene-modified cellulose nanofiber," *Polymer Journal* 51(11), 1189-1195. DOI: 10.1038/s41428-019-0238-8

Suriani, M. J., Ilyas, R. A., Zuhri, M. Y. M., Khalina, A., Sultan, M. T. H., Sapuan, S. M., Ruzaidi, C. M., Wan, F. N., Zulkifli, F., Harussani, M. M., *et al.* (2021). "Critical review of natural fiber reinforced hybrid composites: Processing, properties, applications and cost," *Polymers* 13(20), article ID 3514. DOI: 10.3390/polym13203514

Takeuchi, T., Luengrojanakul, P. L., Ito, H., Rimdusit, S., and Shibata, S. (2023). "Effect of processing temperature and polymer types on mechanical properties of bamboo fiber composites," *BioResources* 19(1), 41-52. DOI: 10.15376/biores.19.1.41-52

Thomason, J. L., and Rudeiros-Fernández, J. L. (2021). "Thermal degradation behaviour of natural fibres at thermoplastic composite processing temperatures," *Polymer Degradation and Stability* 188, article ID 109594. DOI: 10.1016/j.polymdegradstab.2021.109594

Article submitted: December 20, 2024; Peer review completed: March 8, 2025; Revised version received: March 24, 2025; Accepted: March 25, 2025; Published: April 15, 2025.
DOI: 10.15376/biores.20.2.4136-4151